



HAL
open science

Experimental characterisation of flow effects on marine current turbine behaviour and on its wake properties

F. Maganga, G. Germain, J. King, Grégory Pinon, E. Rivoalen

► **To cite this version:**

F. Maganga, G. Germain, J. King, Grégory Pinon, E. Rivoalen. Experimental characterisation of flow effects on marine current turbine behaviour and on its wake properties. *IET Renewable Power Generation*, 2010, 4 (6), pp.498. <10.1049/iet-rpg.2009.0205>. <hal-04496493>

HAL Id: hal-04496493

<https://normandie-univ.hal.science/hal-04496493v1>

Submitted on 22 May 2024

HAL is a multi-disciplinary open access archive for the deposit and dissemination of scientific research documents, whether they are published or not. The documents may come from teaching and research institutions in France or abroad, or from public or private research centers.

L'archive ouverte pluridisciplinaire HAL, est destinée au dépôt et à la diffusion de documents scientifiques de niveau recherche, publiés ou non, émanant des établissements d'enseignement et de recherche français ou étrangers, des laboratoires publics ou privés.



HAL Authorization

Experimental characterisation of flow effects on marine current turbine behaviour and on its wake properties

F. Maganga^{1,2} G. Germain^{1,3} J. King⁴ G. Pinon²
E. Rivoalen⁵

¹IFREMER, Hydrodynamic & Metocean Service, 150 Quai Gambetta, BP 699, F-62321 Boulogne-sur-Mer, France

²Laboratoire Ondes et Milieux Complexes, FRE 3102 CNRS – Université du Havre, 53 rue Prony, 76058 Le Havre, France

³Univ Lille Nord de France, 59000 Lille, France

⁴Engineering Faculty, University of Bristol, Queen's building, Bristol B581TH

⁵Laboratoire de Mécanique de Rouen, Avenue de l' Université, BP 08, 76801 St Etienne du Rouvray

E-mail: ggermain@ifremer.fr

Abstract: Experimental results of tests carried out to investigate the hydrodynamics of marine current turbines are presented. The objective is to build an experimental database in order to validate the numerical developments conducted to characterise the flow perturbations induced by marine current turbines. For that purpose, we used a tri-bladed horizontal axis turbine. The work is dedicated to measuring the behaviour of the system and to characterising the wake generated by the turbine. The efficiency of the device is quantified by the measurement of the thrust and the amount of power generated by the rotor for various inflow conditions, whereas the wake is characterised by Laser Doppler Velocimetry. Particular attention is paid to the flow characteristic effects on the performance of a 0.70 m diameter turbine. The load predictions on the structure and the measured performance of the turbine over its working range of currents and rotational speeds are presented. The results showed that this kind of turbine is sensitive to the quality of the incoming flow. The turbulence intensity effects on turbine behaviour and on its wake are also characterised in order to study how the far wake decays downstream and to estimate the effect produced in downstream turbines.

1 Introduction

The future deployment of marine current energy converters raises questions about their impact on the flow, the interactions with the free surface and the seabed [1, 2]. The question is a timely one, as the first large-scale devices have been installed within the past few years (for example the Marine Current Turbines 1.2 MW 'Sea-Gen' device situated in Strangford Lough, Northern Ireland). In order to quantify these phenomena, numerical tools are being developed in collaboration between Le Havre University and French Research Institute for Exploitation of the Sea (IFREMER) for the characterisation of the impact assessment on the flow of future commercial installations.

Software capable of 3D flow modelling, taking into account the non-stationary evolution of the wake emitted by a tri-bladed horizontal axis turbine is developed in order to assess the effects of disturbances generated on its immediate environment. Currently, we are able to simulate the behaviour of one turbine and to determine the characteristics of the emitted wake [3, 4]. The dynamics of farms consisting of numerous devices placed in arrays will also be analysed. These numerical tools will be used prior to the installation of a marine current turbine farm, with the aim of quantifying the interactions with the immediate environment.

In order to validate this numerical work, experimental trials were carried out in the Ifremer free surface circulation

flume tank. This work is dedicated to measure the behaviour of a tri-bladed horizontal axis turbine and to characterise the wake emitted by its rotor. The behaviour of the turbine is quantified by the measurement of the thrust and the amount of power generated by the rotor for various free-stream flow conditions, whereas the wake is characterised with a 2D LDV system.

Capturing the spatial and temporal variation in the marine flow is vital for the prediction of both performance and loading on marine current turbines. Particular attention is therefore paid to the flow characteristic effects (homogeneous flow, flow with a velocity gradient and flow orientation), and electrical performance results under each of these conditions are compared. We also focus our work on the characterisation of the free stream flow turbulence intensity effects on the performances and on the wake of the turbine. For that purpose we consider two levels of free stream flow turbulence intensity: 8% and close to 25%. These levels of turbulence are investigated here for two purposes:

- to characterise the influence of the choice of the experimental facilities to conduct such trials [5, 6];
- to quantify site characteristic effects on the behaviour of marine current turbine [7, 8].

In this work, both near and far wakes are studied: the near wake characterised by high shear gradient and turbulence intensity, whereas the far wake is characterised by its expansion because of a mix between the wake and the ambient flow. The main interest is to study how the far wake decays downstream, in order to estimate the effect produced in downstream turbines [9, 10].

2 Materials and methods

The turbine used for these trials was developed by Tidal Generation Limited (TGL [11]) before the design of a 500 kW fully submerged tidal turbine prototype, designed for deep water generation. In order to conduct our work at a representative scale and without blockage effects [5], trials were carried out in 2007 on a 1/30th-scale model mounted on a six-component load cells in a ‘free hinge downstream’ configuration. The tri-bladed rotor was connected to a motor–gearbox assembly capable of providing active rotor speed control (gearbox, DC motor, ballast load and motor speed control unit). The pitch of the three blades was adjustable between tests. The diameter of the tested rotor was 0.6 m, which created a blockage ratio (percentage of cross-sectional area occupied by the blades) of approximately 3.5%. The model was tested at speeds ranging from 0.5 to 1.5 m/s and the turbine performances was obtained over a range of rotor speed from 10 to 190 rpm and blades pitch angle from -5 to 15° . The results have been presented in [12].

As intended, the rotor assumed a substantially horizontal orientation when generating. However, although the free hinge downstream testing showed that the turbine was dynamically stable in this configuration across the full range of current and rotational speeds, TGL decided to stop the development of this concept to focus their work on an upstream horizontal axis concept. With this new design, TGL aims to reduce blade loading and achieve better dynamic behaviour.

For this reason it was decided to collaborate on a second set of trials. For these tests, a new 0.7 m diameter (D) tri-bladed horizontal axis turbine (Fig. 1b and Table 1) is used in order to:

- determine the effects of changing flow characteristics (homogeneous flow, flow with a velocity gradient, flow

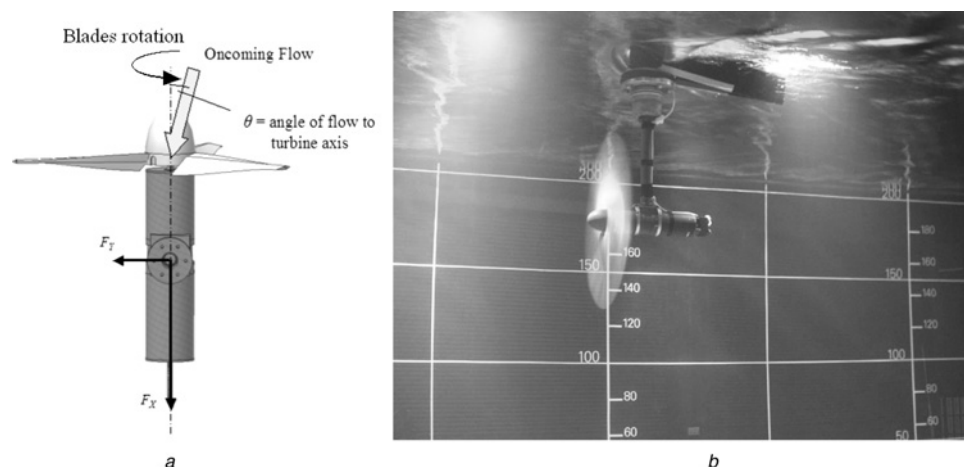


Figure 1 Characteristics of the tri-bladed turbine used during trials

- a* Scheme of the turbine orientation in the tank
b Turbine model testing during trials in the Ifremer tank

Table 1 Turbine model (1/30 scale) specifications used during tests

rotor diameter	700 mm
number of blades	3
Hub height	100 mm
nacelle	400 mm
tower	1100 mm
position of rotor relative to flume tank	upstream
pitch angle	fix at 0°
rotational speed	variable
rotational sense	anti-clockwise
variable current speed	0.5–1.5 m/s

orientation and turbulence intensity) on the operational loads with a six-component load cells;

- characterise the wake of the turbine for different flow conditions (incidence, turbulence intensity and turbine location) with a 2D laser Doppler velocimeter;
- measure the load on an instrumented blade with the use of strain gauges.

Experimental campaigns carried out for this project are performed in the Ifremer free surface hydrodynamic water tunnel (Fig. 2). The flume tank is 18 m long, 4 m wide and 2 m deep with a side observation window of 8 m × 2 m (this large window placed on one side of the tunnel allows users to observe the behaviour of the models during trials and to carry out video sequences). The blockage ratio is then close to 5%. The channel is a closed

loop system with two large variable-speed axial flow pumps providing the thrust to circulate the water with a flow velocity range of 0.1–2.2 m/s. With the use of honeycomb flow straighteners, the free stream flow turbulence is of the order of 8%. Without these flow straighteners, the free stream flow turbulence reaches 25% and can be adjustable with the use of specific grids.

The following instrumentation developed for force, velocity and wave measurements is available:

- three- and six-component load cells with an upper limit of 1500 N for force and 1000 N m for moment measurements;
- two non-intrusive optical measurement devices for flow characterisation: a two-component LDV system for local measurements and a two-component particle image velocimetry (PIV) system in order to obtain global information on the water flow.

The LDV system accurately measures the mean and fluctuating components of fluid velocity. Despite the low data rate obtained in some of the zones being investigated, the data sets allow us to calculate turbulence parameters. The water is seeded with 10 μm diameter polyamide seeding particles and the flow velocity is measured along vertical and/or horizontal profiles. Classical measured velocity components are the axial component (along the x -axis) and the tangential component (along the y -axis, Fig. 1a). This allows us to obtain the flow characteristics all around the majority of the studied devices. The third component (along the z -axis) can be measured separately with the utilisation of a 90° transmitter probe. All this is possible by the use of a three-axis traverse system to move the light source within an accuracy smaller than 0.1 mm. A particular feature of the LDV measurements is that the number of data recorded in a given time window is strongly

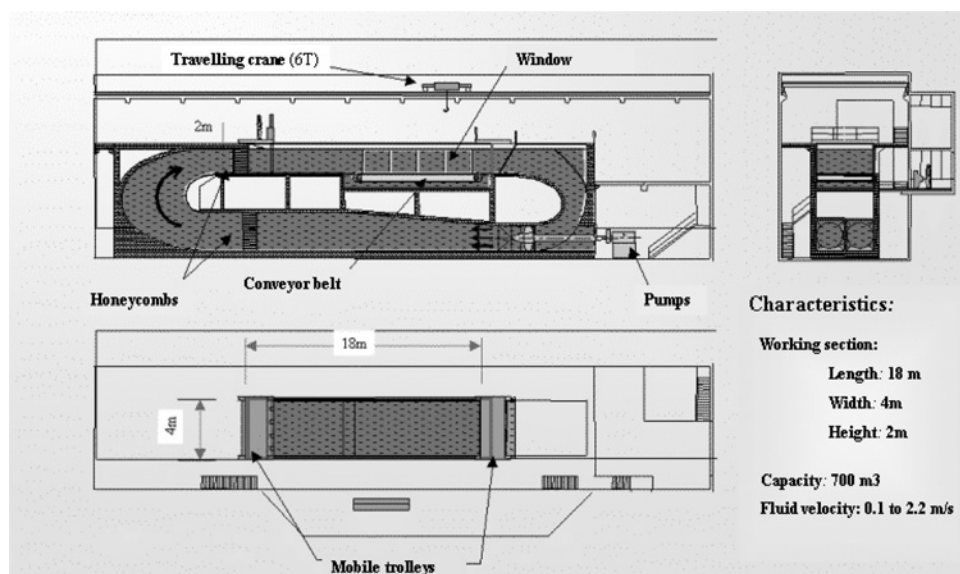


Figure 2 Ifremer free surface hydrodynamic water tunnel located in Boulogne-sur-Mer, France

dependent on the local seeding conditions [12]: measurements are possible only when a particle is moving across the probe volume. So the data rate is generally of the order of 50 Hz. In order to achieve samples of data as homogeneous as possible, an inhibition method is used and data are recorded under time rather than sample length control. This technique allows us to obtain a sample length of the order of 100 s (that is an order of magnitude for the time window larger than the time scale of the flow fluctuations) with a number of data per sample of the order of a few thousand. The long time interval allows an accurate estimate of average values, both for velocity and for turbulence intensity [13].

The LDV system is also used to determine and verify the quality of the flow in the tank. From the resulting flow maps obtained without any device in the test section, we can extract the dispersion of the axial velocity: for a mean axial velocity value of 0.79 m/s, the axial mean velocity variations are lower than 2% in the central part; with a turbulence intensity rate close to 8%, value is calculated as follows

$$TI = 100 \times \frac{\sqrt{(\sigma_u)^2 + (\sigma_v)^2 + (\sigma_w)^2}}{\sqrt{u^2 + v^2 + w^2}}$$

giving a relative measure of turbulence (σ indicates standard deviation, and u , v and w are average fluctuating components of fluid velocity, respectively, in the x , y and z directions).

From these data, it is also possible to quantify the power P available from the flow through the rotor area: $P = (1/2)\rho S U^3$, where ρ is the density, S the cross-sectional area of the turbine and U the current speed over S , and to determine the turbine performance in terms of power and thrust coefficients

$$C_p = \frac{P}{(1/2)\rho S U^3}$$

and

$$C_T = \frac{T}{(1/2)\rho S U^3}$$

where C_p and C_T are, respectively, the output power and the thrust coefficients. For example, at a nominal flume speed of 0.8 m/s, the available power from the flow through the rotor area for the homogeneous flow with an ambient turbulence intensity rate close to 8% is 92 W. For the left to right transverse velocity gradient flow with an ambient turbulence intensity rate close to 8% the available power is 104 W, and 78 W for the flow with an ambient turbulence intensity rate close to 25% (measurements carried out without the turbine in the tank). This kind of data (velocity map) is also used to characterise the wake of the turbine in order to evaluate the flow perturbation and to develop a database for numerical validations. During trials, the time

history data of the flow speed at the centre of the tank is recorded and synchronised with power measurements in order to characterise precisely the response of the system.

3 Data presentation

The objective here is merely to give some comparisons between configurations and to determine some possible effects on the turbine behaviour. Owing to the confidential and commercially sensitive nature of the results, the following results are presented as raw data. Curves are presented as function of the tip speed ratio (the rotor speed divided by the oncoming flow speed) or frequency multiplied by an unspecified factor in order to further protect the confidentiality of the data: $TSR^* = (\Omega D/2U_\infty) \times A$ and $F^* = F \times B$, with the coefficients A and B not given here.

Horizontal axis rotor wake recovery is defined in terms of velocity deficit, which is relative to the free-stream flow speed (U_∞) and the wake velocity at rotor centreline (U_c)

$$U_{\text{def}} = 1 - \frac{U_c}{U_\infty}$$

4 Results and discussion

4.1 Turbine behaviour for various flow characteristics

In order to study the impact varying flow characteristics can have on a tri-bladed horizontal axis turbine, the performance of the turbine over a range of common rotor speeds and a range of mean flow speeds between 0.5 and 1.5 m/s are measured for:

- three kinds of flow: a homogeneous one (with a turbulence intensity rate of 8%), a flow with a transverse velocity gradient (left to right gradient of 8%) and a flow with an intermediate turbulence intensity rate of 25%;
- three locations in the tank: turbine axis position located at $0.94D$, $1.57D$ and $2.04D$ from the free surface. The depth location of reference is the mid-depth location of $1.57D$ from the free surface.

From these results, the mathematical data obtained by TGL from a model based on the blade element momentum theory can be validated [12]. The principle of this theory is to combine the momentum and the blade element theories for predicting the performance of the turbine and the blade loadings. Fig. 3 shows the measured electrical power generated by holding at a specific constant rotational speed of the turbine (by dissipating power through load resistors) for both a homogeneous flow and a flow with a transverse gradient of 8%. The power values given here take into account the losses in the gearbox and the inefficiencies of the motor itself. Results show a similar

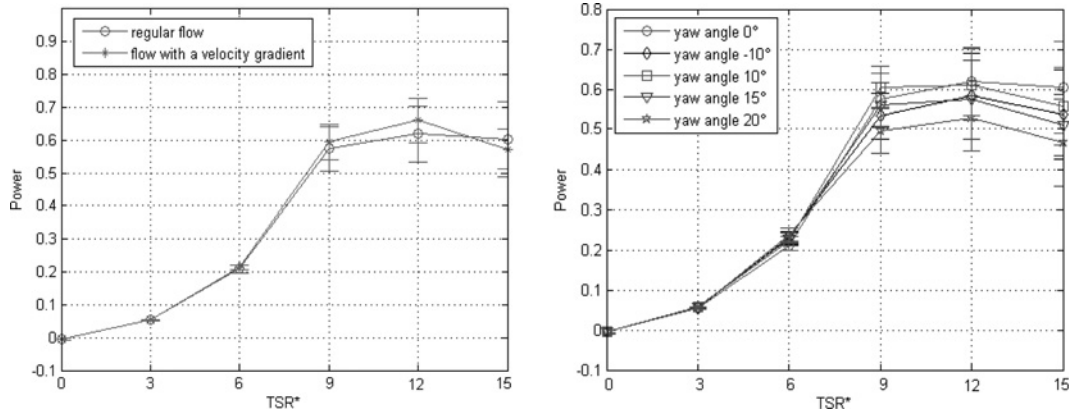


Figure 3 Measured power for a homogeneous flow and a flow with a left-to-right velocity gradient (on the left) and for different yaw angles (on the right) at a mid-depth location with a mean flow velocity of 0.8 m/s

response of the turbine for both configurations. From earlier calculations, the difference in theoretically available power between both configurations reaches 10%. However, this difference is surprisingly not visible on the measured power given here. If this cannot be explained, it is evident from these results that this kind of system is less efficient when it is in presence of non-homogeneous flow. No more sensitive effects can be seen on the thrust on the rotor for each configurations, even if the thrust fluctuations are always lower for the flow with a gradient than for the homogeneous one (certainly because of the higher flow speed on one side of the rotor disc). Some characteristics of the wake generated by the turbine in these different configurations should give additional information in order to try to understand these phenomena, both for the kind of flow or location of the turbine in the tank.

Moreover, a similar response is obtained from the comparison between depth locations, but from the results given in [14] we might think the opposite. The theoretical available power is equivalent for the three locations. If there are some effects on the emitted wake, it seems not to affect the behaviour and performance of the turbine. During the

next experimental campaign we will increase the flow gradient in order to improve these results and to determine the point at which significant changes occur. These new configurations will be obtained with a location of the turbine close to the bottom of the tank (in the boundary layer): by doing this, we will be able to produce a variation in flow velocity of 20% across the blades.

Not only is the influence of the yaw angle on the thrust, the rotor torque and the power is studied in order to characterise the effects of a misalignment during installation but also the effects of variations of the flow direction during the reverse of the current or during a tide cycle. It can be seen on thrust graph (Fig. 4) some small effects for a variation of $\pm 10^\circ$. For orientation higher than 10° , the thrust losses are significant: of the order of 15%. The variations of the torque imposed by the rotor on the turbine as a function of the alignment of the turbine correspond more closely to what was expected: a decrease in torque with the reduction of the quantity of flow seen by the blades and the behaviour of the flow around the blades. The loads on the blades present a significant gap between the orientations -10° and 10° , whereas the thrust seems to be not

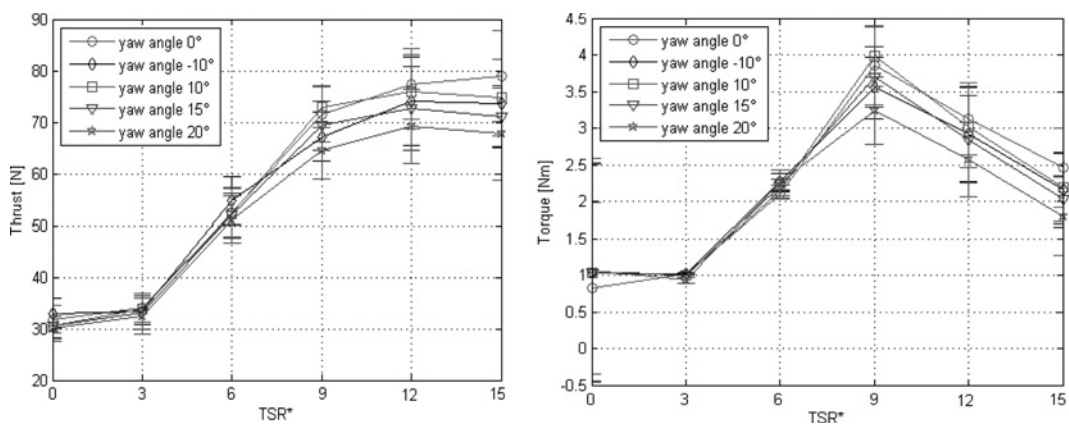


Figure 4 Measured thrust (left) and rotor torque (right) for several turbine orientations at a mid-depth location and a mean flow velocity of 0.8 m/s

influenced by the incidence of the flow. Some PIV measurements of tip flow and vortices and load measurements on an instrumented blade with the use of

strain gauges will be done through future work in order to study this point. Fig. 3 shows the measured power generated by holding the turbine at a specific constant

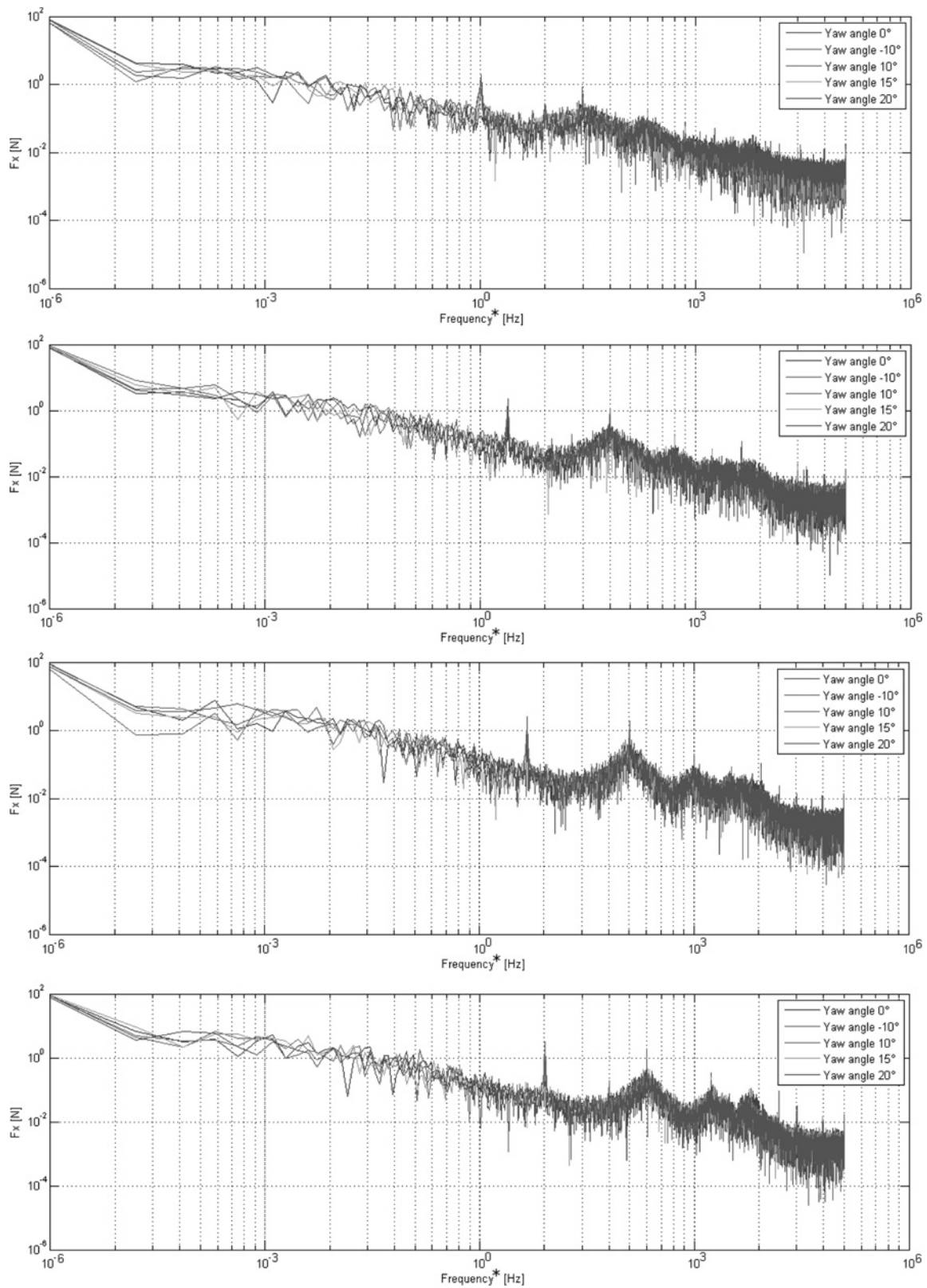


Figure 5 Axial force spectrums for four rotor speeds and five turbine orientation angles in the flow between -10 and 20° (increasing TSR^* from the top to the bottom from 9 to 18) at a mid-depth location and a mean flow velocity of 0.8 m/s

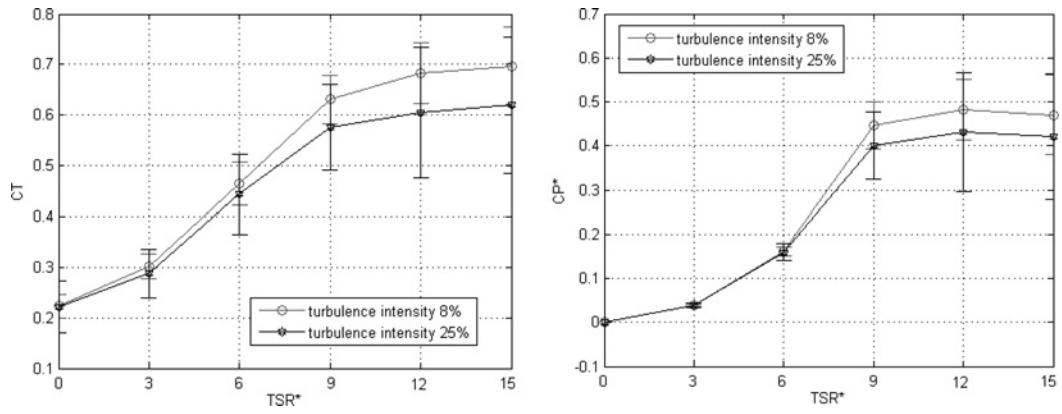


Figure 6 Thrust (left) and power (right) coefficients for ambient turbulence intensity levels of 8 and 25% at a mid-depth location and a mean flow velocity of 0.8 m/s

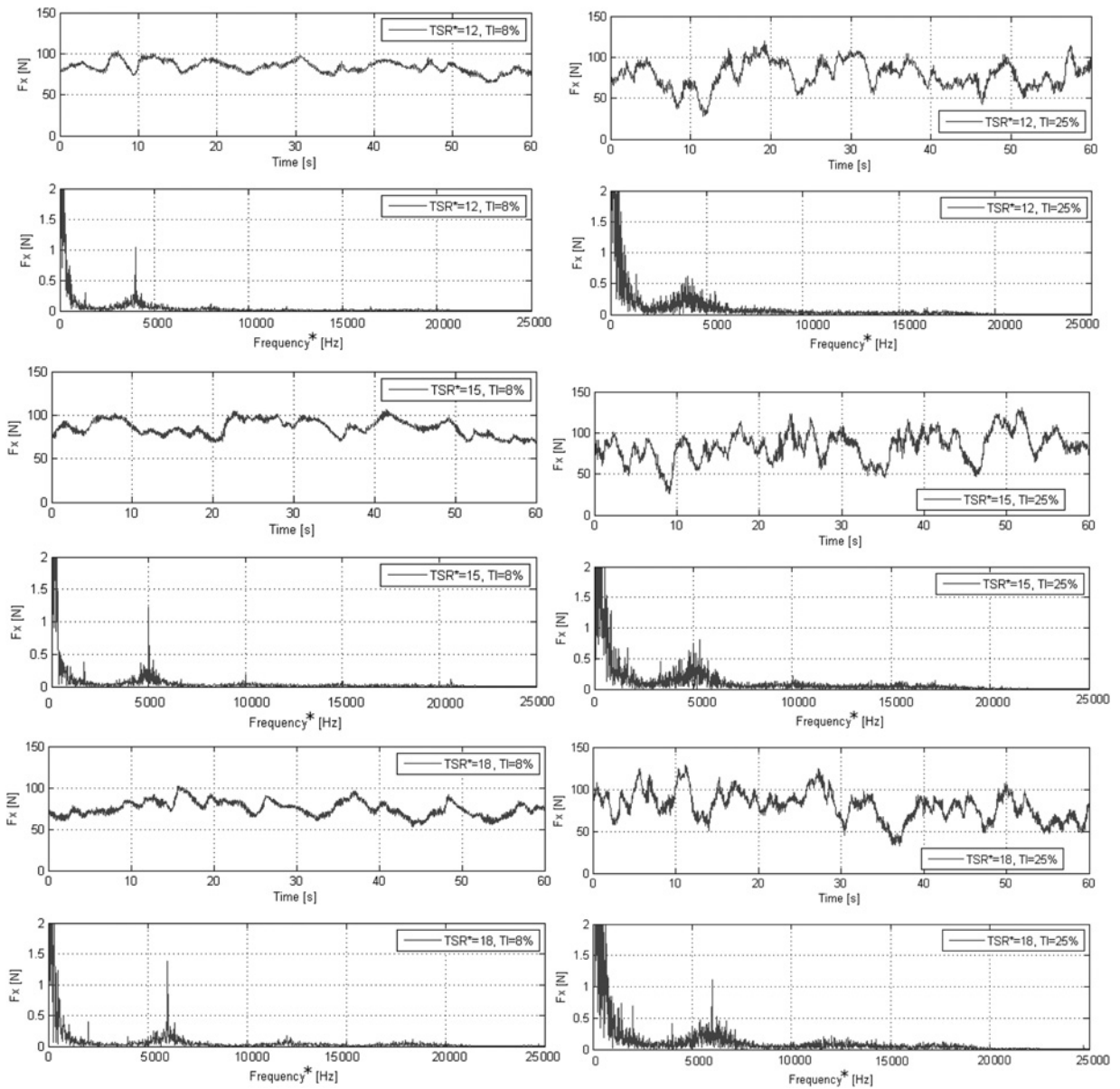


Figure 7 Axial force spectra and time history for two turbulence intensity levels, that is, 8 and 25% and 3 TSR^* at a mid-depth location and a mean flow velocity of 0.8 m/s

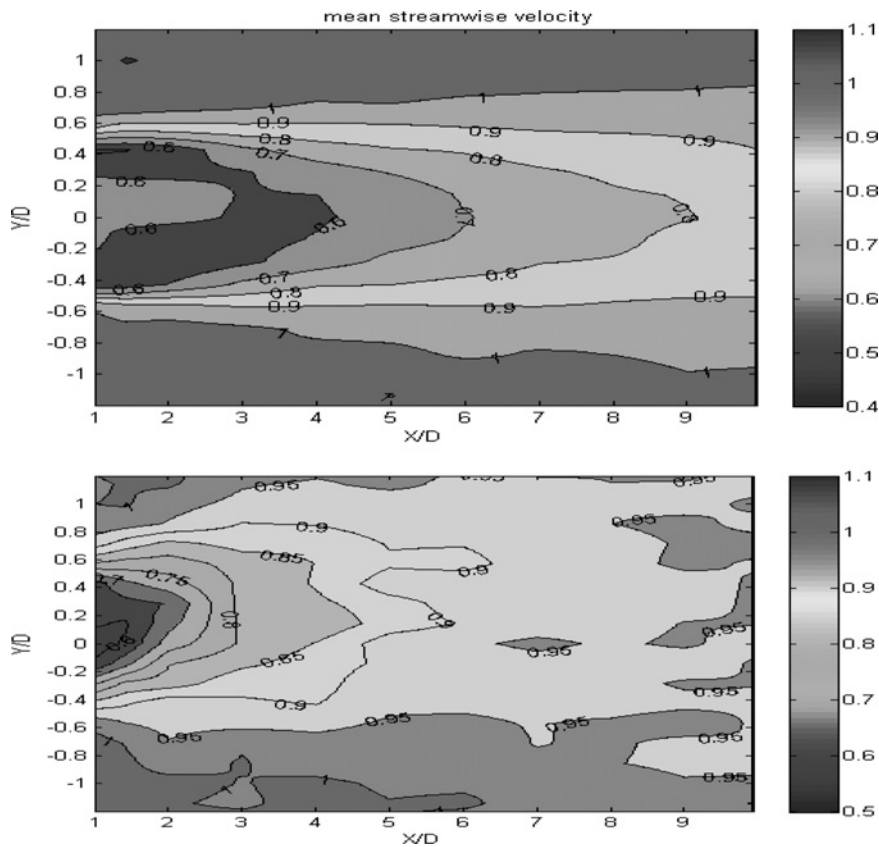


Figure 8 Contours of mean streamwise velocity deficit at $TSR^* = 18$ for the two turbulence intensity levels (8% at the top and 25% at the bottom)

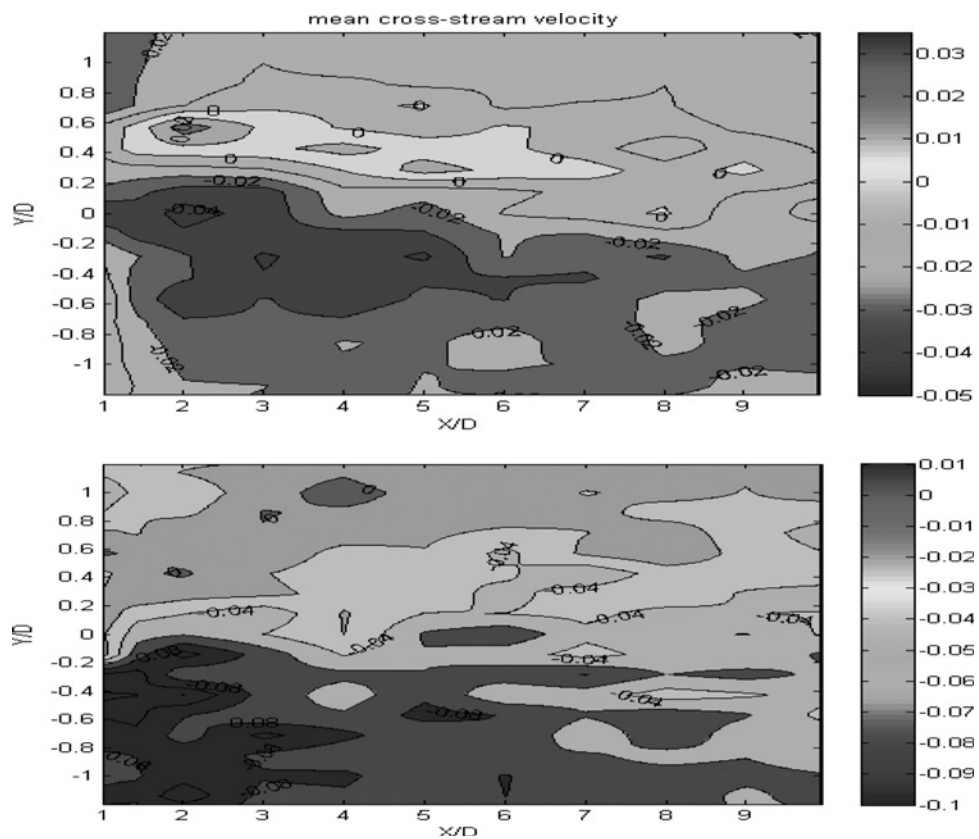


Figure 9 Contours of cross-stream velocity deficit at $TSR^* = 18$ for the two turbulence intensity levels (8% at the top and 25% at the bottom)

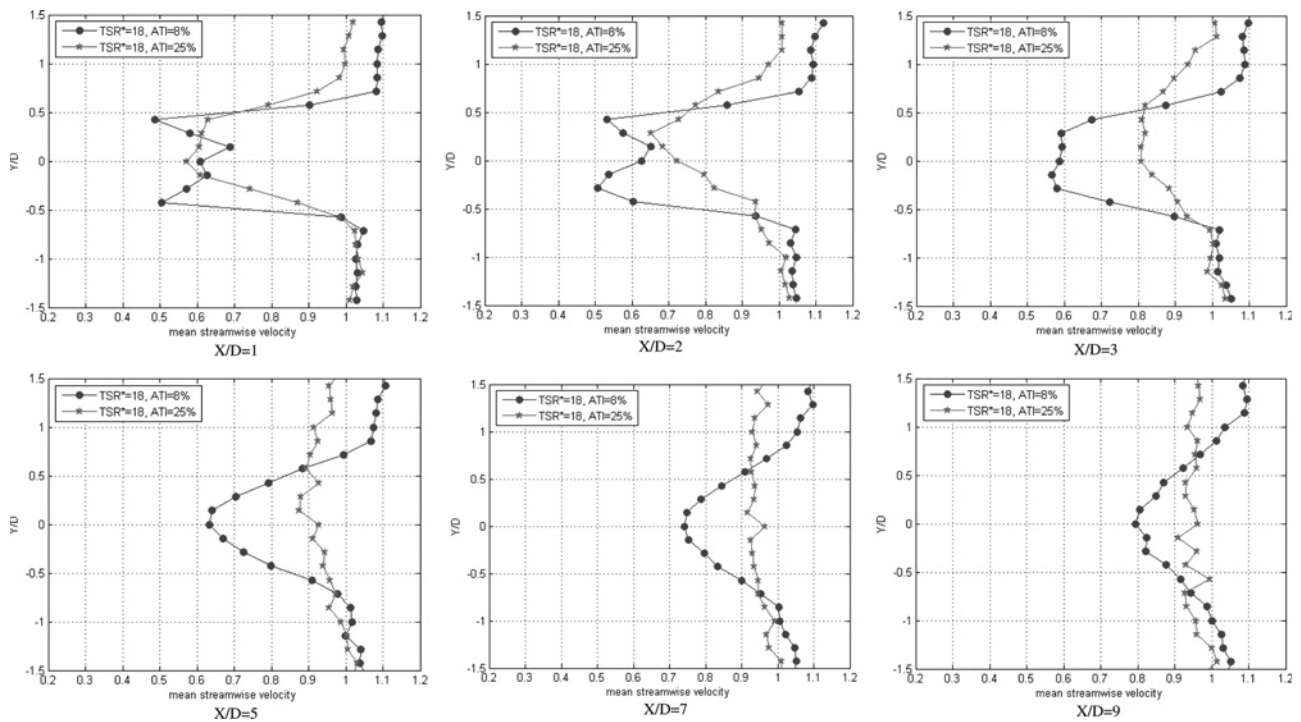


Figure 10 Mean streamwise velocity for two ambient turbulence intensities at $TSR^* = 18$ for $X/D = 1-9$

rotational speed for the five turbine alignment angles investigated. A misalignment of -10° of the turbine can cause significant losses whereas a misalignment of 10° seems to be not significant. The effective angle of incidence of the flow on the blades is not altered in the same way by the orientation of the turbine. The interaction between the wake of the blades and the tower is also not similar in both cases. It can be seen clearly in Fig. 4 that the thrust drops as the yaw angle increases.

In order to complete the analysis of the force measurements and to determine the structural response of the structure, the axial force spectra for four rotor speeds and five yaw angles (between -10 and 20°) are presented in Fig. 5. The axial force spectra do not show any significant differences between the different orientation angles, but they give the rotational frequency of the rotor (first peak at f_0) and the response of the blades passing the tower (second peak at $3f_0$) and its harmonics for each TSR^* . The maximal response (energy level) is obtained here when the maximum performance is achieved. At both sides of this point (at lower and higher tip speed ratio), the harmonics become more clearly defined.

During these trials, the influence of the ambient turbulence intensity on the performances of the turbine was studied. For that purpose we have considered two levels of turbulence intensity rates: close to 8% and close to 25%. As it can be seen in Fig. 6, the behaviour of the turbine is the same for both kinds of flow. The C_p and C_T curves present significant losses of the order of 9% from $TSR^* = 9$ for the higher turbulence intensity flow rate. As expected, the

thrust fluctuations are always higher for the higher turbulence rate than for the smaller one: double for the 25% turbulence intensity rate compared to the 8% one. If, like shown in [15], the force oscillations on the turbine are three times greater than the force oscillations for the three blades (as given here) because of the level of velocity fluctuation, it could be a useful determinant for the fatigue loading on the blades. The available power from the flow through the rotor area for a turbulence intensity rate of 25% is 15% lower than that of the reference flow (flow with ambient turbulence rate of 8%). If we compare the electric output power after mechanical losses for both intensity rates (given Fig. 6), we find a difference of less power than expected: 9% compared to the previous 15%. Fig. 7 shows the axial forces spectrum for the two turbulence intensity rates. A load change towards a higher power spectral density level for all frequencies is observed, reflecting the increased turbulence intensity of the flow. These results highlight the high level of the loading fluctuations on the structure [16].

4.2 Velocity distribution in the wake of a single turbine

The wake of a turbine can be divided into a near and a far wake regions. The characterisation of the near wake is essential to improve the performances and the physical process of power extraction, whereas the far wake characterisation is a key to minimise the mutual influence of turbines placed in arrays. In this case, the incident flow over the affected turbines has a lower velocity and a higher turbulence intensity. In order to increase our knowledge of

induced turbine behaviour, we have made flow measurements for two turbulence intensity rates of 8 and 25%. Velocity measurements have been performed using the 2D LDV system in the horizontal plain at the centre of the tri-bladed turbine. The velocity components were measured at 25 probe locations in transverse direction from $Y = -1.7$ to $+1.7D$ with a space step of 10 cm. Ten locations in the wake of the turbine were considered in the range $X = 1$ to $10D$ with a space step of 0.7 m.

Mean streamwise velocity distribution of a single tri-bladed horizontal axis turbine for two ambient turbulence rates at a mid-depth location in the tank is shown in Fig. 8. It shows the extension and the decay of the wake velocity deficit. We observe a faster recovery of the flow in the area of greater ambient turbulence intensity. After $5D$, the velocity deficit in the wake of the turbine is almost negligible for the flow with the ambient turbulence intensity of 25%, whereas the velocity deficit is clearly present more than $10D$ downstream for the flow with turbulence intensity of 8%. The extension of the wake in the cross-flow direction is large as well as the turbulence level is significantly high. These results confirm experimental studies of several authors [17–20] on the

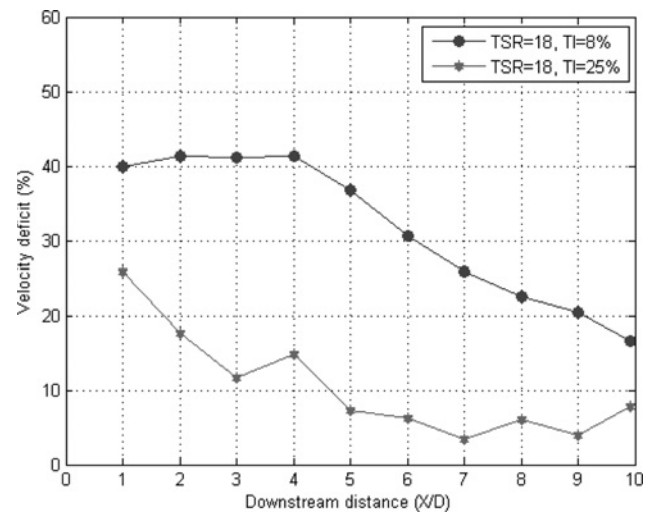


Figure 11 Mean centreline streamwise velocity deficit for two ambient turbulence intensities at $TSR^* = 18$

influence of ambient turbulence intensity on the near wake of wind turbine, the circular cylinder or a prism. The maximum decay of the wake velocity deficit is close to 60% until $4.4 D$ downstream the turbine for $TI = 8\%$, whereas is close to 60%

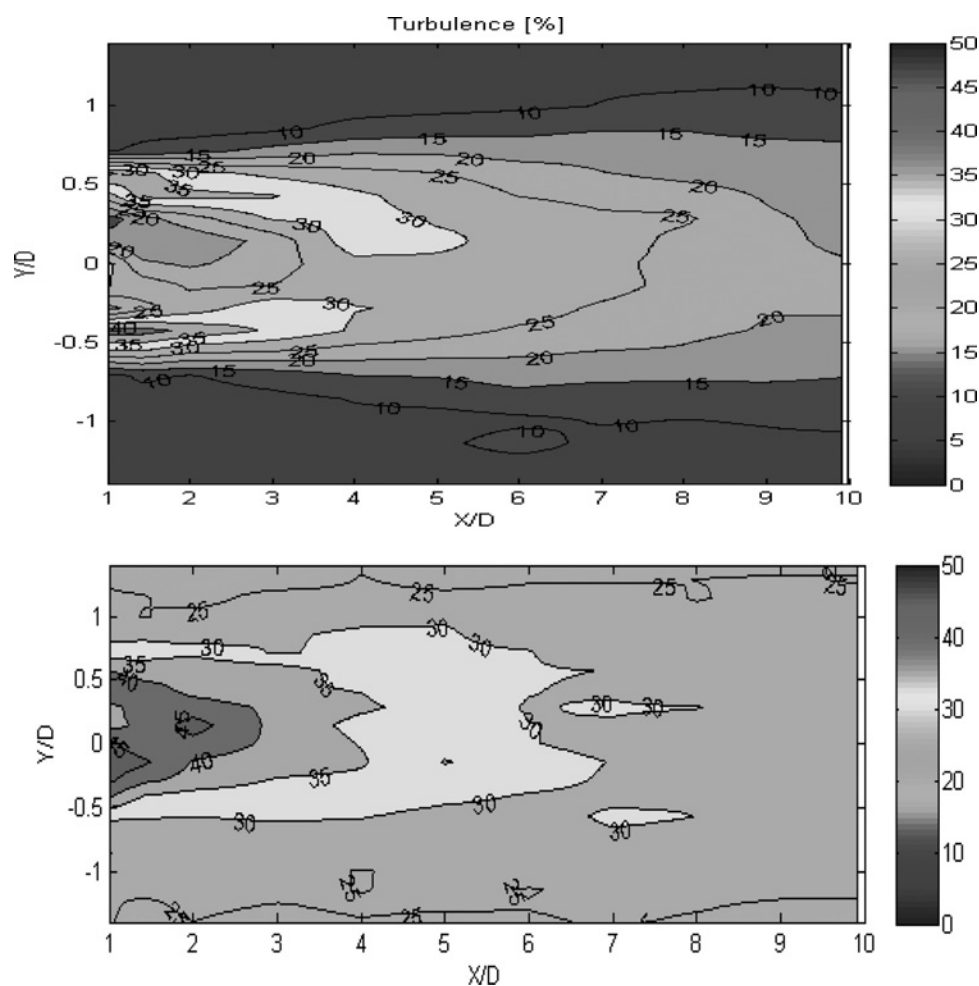


Figure 12 Contours of turbulence intensity for $TSR^* = 18$ for two ambient turbulence intensity levels (8% at the top and 25% at the bottom)

until $1.4D$ for $TI = 25\%$. A decay of 80% in the wake velocity deficit for water streamwise velocity is obtained (for an ambient turbulence intensity of 8%) at $9D$ downstream, whereas it is obtained before $3D$ for $TI = 25\%$. The transverse mean velocity component (Fig. 9) is of opposite sign on the two sides of the wake because of the continuity condition. Contrary to wind turbine [21, 22], this effect is relatively small and restrained to the wake deficit region. Transverse velocity will be investigated further with the PIV system in order to understand the location of vortex structures in the near and the far wake [23].

Mean velocity profiles measured at six streamwise locations in the horizontal symmetry plane of the turbine are plotted in Fig. 10 for both flows (turbulence intensities of 8% and 25%). The results show the high perturbation level on the near wake (from $X/D = 1-3$) at $TI = 8\%$ because of the hub, turbine body and supporting structure. For a turbulence intensity of 25% these effects are not noticeable, essentially because of the high velocity deficit decrease (Fig. 11) and to the non-development of the wake of the hub. In the far wake, starting at $X/D \sim 2$ for the high turbulence intensity and $X/D \sim 5$ for the lower one, the classical Gaussian shape is observed. The evolution of the mean centreline streamwise velocity deficit for $TI = 8\%$ is qualitatively equivalent to the one reported in [24], but with lower values of more than 10%, whereas the velocity deficit for $TI = 25\%$ becomes negligible very quickly.

From these results, it is clear that wakes of marine current and wind turbines present similar characteristics [18, 25]. A direct comparison is not really possible because of the high dependence level of the wake development with the used parameters, essentially with the thrust coefficient of the turbine and the turbulence intensity level of the flow [25]. This dependency is clearly put in evidence in Fig. 12, where the evolution of the turbulence intensity evolution is given for $TI = 8$ and 25% at $TSR^* = 18$. The peak of turbulence intensity occurs before $3D$, with a turbulence intensity of 40 and 45%, respectively, for $TI = 8$ and 25%, because of the increase in turbulence energy dissipation from the near wake. The turbulence intensity level is relatively high compared to that obtained behind a wind turbine (less than 25% in the last case [18]). The helical vortex originating from each blade can be well seen for $TI = 8\%$. These helical tip vortices are convected downstream with the local flow velocity and form a continuous vortex layer that produces a shear layer in the wake near the end blade location with a strong turbulent intensity with respect to the inner region of the wake. Turbulence effects are more persistent for low ambient turbulence intensity level than for the higher one.

5 Conclusions

Successful measurements of the performance characteristics of a tri-bladed horizontal axis turbine have been conducted in a free surface circulation tank. A specific assembly has

been designed and a test programme carried out that provided satisfactory results and suitable data for validating theoretical and numerical methods.

The experimental results shown that a misalignment of a fixed turbine can cause a significant loss of thrust and power. The characterisation of the influence of the ambient turbulence intensity rate on the behaviour of the turbine was studied. It reveals high loading fluctuations on the blades for the flow with a greater ambient turbulence intensity. This study should be extended in order to evaluate the impact that the high loading fluctuations on the blades could have on the fatigue of the structure.

The flow measurements for wake effects characterisation were also performed for two ambient turbulence intensities. It was observed (as expected) that the water velocity recovery is faster in area of greater ambient turbulence intensity. Increased ambient turbulence intensity leads to the formation of a narrower wake (streamwise direction). Rapid changes in turbulent kinetic energy production and rates were also observed and particularly putting in evidence in the near wake region. Flow particularities like the level of homogeneity, the variations of the orientation and the rate of the turbulence should be properly considered for the characterisation of the turbine behaviour and the wake properties. Thus, the need to conduct experimental trials in adapted facilities is therefore of great importance. Further development should be carried out to simulate more realistic sea states (wave effects), as in [7]. For that purpose, combined trials with waves and current will be carried out in the Ifremer flume tank in the future.

6 Acknowledgments

The authors wish to thank the Région Haute-Normandie for the financial support (co-financing of the PhD) of this collaborative work with TGL carried out in the Ifremer flume tank. We also would like to acknowledge and thank J.V. Facq and B. Gaurier for their implication in the project.

7 References

- [1] MYERS L., BAHAJ B.: 'Scale reproduction of the flow field for tidal energy converters'. WREC X, Glasgow, 2008
- [2] MYERS L., BAHAJ B.: 'The effect of boundary proximity upon the wake structure of horizontal axis marine current turbines'. 27th OMAE, Estoril, June 2008
- [3] MAGANGA F., PINON G., GERMAIN G., RIVOALEN G.: 'Numerical simulation of the wake of marine current turbine with a particle method'. WREC X, Glasgow, 2008
- [4] MCCOMBES T., JOHNSTONE C., GRANT A.: 'Unsteady 3d wake modeling for marine current turbines'. Eighth EWTEC, Uppsala, Sweden, 2009

- [5] GERMAIN G.: 'Marine current energy converter tank testing practices' (ICOE, Brest, 2008)
- [6] BAHAJ A.S., MYERS L.E., THOMSON M.D., JORGE N.: 'Characterising the wake of horizontal axis marine current turbines'. Proc. Seventh European Wave and Tidal Energy Conf., Porto, Portugal, 2007
- [7] MASTERS I., ORME J.A.C., CHAPMAN J.: 'Towards realistic marine flow conditions for tidal stream turbine'. Seventh EWETEC, Porto, September 2007
- [8] GUINOT F., LE BOULLUEC M.: 'Realistic marine flow conditions for current turbines studies'. Second ICOE, Brest, France, 2008
- [9] BAI L., SPENCE R.R.G., GRÉGORY D.: 'Investigation of the influence of array arrangement and spacing on tidal energy converter (TEC) performance using a 3-dimensional CFD model'. Eighth EWTEC, Uppsala, Sweden, 2009
- [10] LISSAMAM P.B.S.: 'Energy effectiveness of arbitrary arrays of wind turbines'. AIAA paper 79-0114, 1979, pp. 1–7
- [11] <http://www.tidalgeneration.co.uk/>
- [12] GERMAIN G., BAHAJ A.S., ROBERTS P., HUXLEY-REYNARD C.: 'Facilities for marine current energy converter characterization'. Seventh EWETEC, Porto, September 2007
- [13] PICHOT G., GERMAIN G., PRIOUR D.: 'On the experimental study of the flow around a fishing net', *Eur. J. Mech. B. Fluids*, 2009, **28**, pp. 103–116
- [14] MYERS L., BAHAJ B., GERMAIN G., GILES J.: 'Flow boundary interaction effects for marine current energy conversion devices'. WREC X, Glasgow, July 2008
- [15] BATTEN W.M.J., BAHAJ A.S., MOLLAND A.F., CHAPLIN J.R.: 'The prediction of the hydrodynamic performance of marine current turbines', *Renew. Energy*, 2008, **33**, (5), pp. 1085–1096
- [16] SORENSEN P., HANSEN A., JANOSI L., BECH J., BAK-JENSEN B.: 'Simulation of interaction between wind farm and power system'. Riso R-1281, 2001
- [17] ADRARAMOLA M.S., AKINLADE O.G., SUMNER D., BERGSTROM D.J., SCHENSTEAD A.J.: 'Turbulence wake of a finite circular cylinder of small aspect ratio', *J. Fluids Struct.*, 2006, **22**, pp. 919–928
- [18] VERMEER L.J., SØRENSEN J.N.S., CRESPO A.: 'Wind turbine wake aerodynamics', *Prog. Aerosp. Sci.*, 2003, **39**
- [19] DEVARAKONDA R., HUMPHREY J.A.C.: 'Turbulent flows in the near wakes of prism', *Heat and Fluid Flow*, 1996, **3**
- [20] WUBOW S., SITZKI L., HAHM T.: '3D-simulation of the turbulent wake behind a wind turbine', *J. Phys. Conf. Ser.*, 2007, **75**
- [21] SØRENSEN J.N.S., SHEN W.Z.: 'Numerical modelling of wind turbine wakes', *J. Fluids Eng.*, 2002, **124**
- [22] CRESPO A., MANUEL F., MORENO D., FRAGA E., HERNANDEZ J.: 'Numerical analysis of wind turbine wakes'. Proc. Delphi, Greece, 1985
- [23] GRANT I., MO M., PAN X., ET AL.: 'An experimental and numerical study of the vortex filaments in the wake of an operational, horizontal-axis, wind turbine', *J. Wind Eng. Ind. Aerodyn.*, 2000, **85**, pp. 177–189
- [24] MYERS L., BAHAJ A.S.: 'Near wake properties of horizontal axis marine current turbines'. Eighth EWTEC, Uppsala, Sweden, 2009
- [25] EL KASMI A., MASSON C.: 'An extended $\kappa-\varepsilon$ model for turbulent flow through horizontal-axis wind turbines', *J. Wind Eng. Ind. Aerodyn.*, 2008, **96**, pp. 103–122